

Picosecond energy-relaxation processes of excitons in CdSe

Yasuaki Masumoto and Shigeo Shionoya

*The Institute for Solid State Physics, The University of Tokyo,
Roppongi 7-22-1, Minato-ku, Tokyo 106, Japan*

(Received 23 January 1984; revised manuscript received 4 May 1984)

Energy- and time-resolved luminescence of the one longitudinal optical-phonon Stokes sideband of the A exciton in CdSe has been studied in the picosecond time domain under the weak band-to-band excitation. Dynamic energy relaxation of excitons is directly visualized in the energy-time coordinates. The observed energy-relaxation rate of excitons is explained by a model taking into account three types of exciton-phonon interactions, that is, the deformation-potential-type, the piezoelectric-type, and the Fröhlich-type interaction. This result clearly demonstrates the applicability of the method used in this work to the analysis of the energy relaxation of excitons.

Recent advances of picosecond spectroscopy have enabled us to observe directly dynamic energy-relaxation processes of excitons.¹⁻⁴ In semiconductors the energy relaxation of excitons is considered to occur via three types of exciton-phonon interactions. They are the deformation-potential-type, the piezoelectric-type, and the Fröhlich-type interactions. However, so far there have been scarcely any experimental studies to reveal the role of these interactions in the energy relaxation of excitons.

In the present work the energy- and time-resolved luminescence of the one longitudinal optical-phonon (LO) Stokes sideband of the A exciton (A -LO) in CdSe is examined with picosecond time resolution under the rather weak band-to-band excitation. Because of the polariton effect, the luminescence line shape of the A -exciton zero-phonon band is related to the energy distribution function of excitons in a rather complicated manner. On the other hand, the line shape of the A -LO band directly reflects this distribution function.⁵ Therefore, the analysis of the A -LO band is more favorable than that of the zero-phonon band to derive the distribution function. The group velocity of the excitonic polaritons in the A -LO band region is so fast ($\frac{1}{3}$ of the light velocity in vacuum) that the time-resolved A -LO luminescence quickly follows the time evolution of the energy distribution of excitons. From the time evolution of the distribution thus observed, we clarify the role of the exciton-phonon interactions in the energy relaxation of excitons.

A platelet-type CdSe crystal was grown by the vapor-transport method. The crystal, having the c axis lying in its face, was directly immersed in liquid helium. Light pulses given by a Rhodamine-6G dye laser synchronously pumped by a mode-locked argon laser were used as the excitation source. Laser light with a pulse width of 1–2 ps and the output of 300 pJ/pulse was focused on the face of the CdSe crystal with the spot diameter of 200 μm . The lasing photon energy, 2.072 eV, with the spectral width of 2 meV corresponds to the band-to-band excitation of CdSe.

The spectrally resolved temporal response of the luminescence was analyzed by using a system consisting of a 25-cm monochromator, a synchroscan streak camera (HTV-C1587), a silicon intensifier target (SIT) camera, and a computer. The spectral resolution was 1.4 meV. The time resolution of the combined system of the laser, the monochromator, and the streak camera was 70 ps, which is deter-

mined by the jitter and the finite slit width of the streak camera and the spread of the light path in the monochromator. Another 50-cm monochromator and an intensified SIT camera were used to obtain the time-integrated luminescence spectra with the spectral resolution of 0.2 meV.

In Fig. 1, time-integrated luminescence spectra of the A -exciton band and the A -LO sideband are shown. Under the

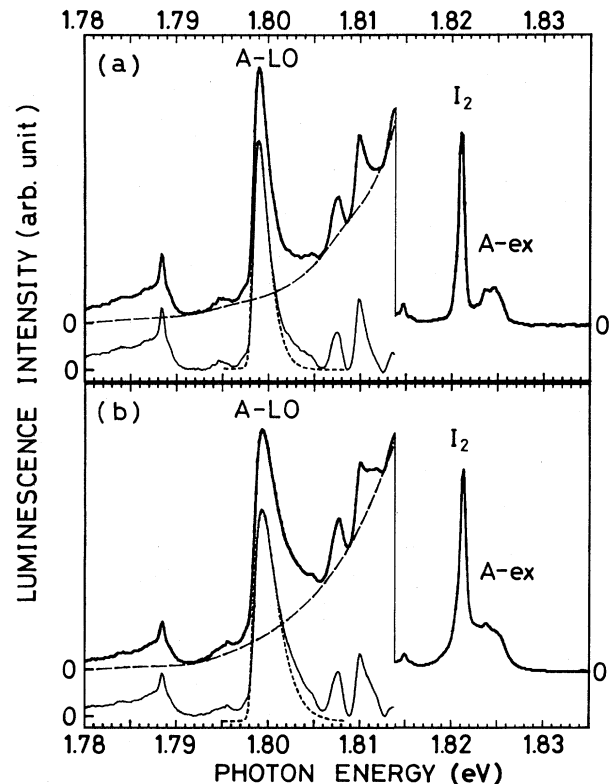


FIG. 1. Time-integrated luminescence of the A -exciton and A -LO bands of CdSe (a bold line) at 4.2 K under the irradiation of (a) the cw He-Ne laser (1.959 eV, 1 mW) and (b) the pulsed dye laser (2.072 eV, 1–2 ps, 300 pJ). The spectral resolution is 0.2 meV. Dashed lines show smooth backgrounds assumed and fine lines show the luminescence structures obtained by subtracting the backgrounds from the luminescence spectra. Theoretical fits on the basis of Eq. (2) are shown by dotted lines, assuming $T_e = 9$ K for (a) and 14 K for (b).

excitation of the 1–2-ps (300-pJ) light pulses, the A -exciton and A -LO luminescence bands [Fig. 1(b)] are broadened compared with those under the excitation of 1-mW He-Ne cw laser light [Fig. 1(a)]. The line shapes of the A -LO and A -2LO bands have been considered to be expressed by

$$(\tilde{E} - E_t + E_{LO})^{3/2} \exp[-(\tilde{E} - E_t + E_{LO})/k_B T_e]$$

and

$$(\tilde{E} - E_t + 2E_{LO})^{1/2} \exp[-(\tilde{E} - E_t + 2E_{LO})/k_B T_e],$$

respectively.^{5,6} Here, \tilde{E} is the luminescence photon energy, E_t ($=1.8242$ eV)⁷ the transverse A -exciton energy, E_{LO} ($=26.3$ meV)⁷ the LO-phonon energy, and T_e the effective time-averaged temperature of the exciton ensemble. The line shape of the A -2LO band directly reflects the Maxwell-Boltzmann distribution of excitons. On the other hand, the line shape of the A -LO band reflects on both the energy distribution and the q dependence of the matrix element of the Fröhlich-type $1s$ exciton-LO-phonon interaction,⁸

$$V_F(q) = (1/q) [(2\pi E_{LO} e^2 / V) (1/\epsilon_\infty - 1/\epsilon_0)]^{1/2} (q_e - q_h), \quad (1)$$

where

$$q_e (q_h) = \{1 + [(qa_B/2)m_{h(e)}/(m_e + m_h)]^2\}^{-2}.$$

q is the wave vector of phonons, V the volume of the crystal, e the charge of an electron, $\epsilon_{\infty(0)}$ the optical (static) dielectric constant, $m_{e(h)}$ the mass of an electron (hole), and a_B is the Bohr radius of the $1s$ exciton. The extra factor $(\tilde{E} - E_t - E_{LO})$ in the line shape of the A -LO band arises from the asymptotic form ($q \rightarrow 0$) of the matrix element, noting that

$$(1/q)(q_e - q_h) \approx (qa_B^2/2)(m_e - m_h)/(m_e + m_h)$$

when $q < 1/a_B$. This usual line-shape analysis includes a flaw, because the T_e obtained for the A -LO band was found to be slightly lower than that for the A -2LO band. This discrepancy is considered to arise because the condition $q < 1/a_B$ does not hold at the high-energy side of the A -LO band.

For the refined line-shape analysis, we take the following procedure. In the procedure the polariton effect as well as the accurate q dependence of the Fröhlich-type interaction are taken into consideration. Excitons are assumed to be populated on the following polariton dispersion obeying the Boltzmann distribution $\exp(-E/k_B T_e)$.

$$(\hbar ck/E)^2 = \epsilon(k, E) = \epsilon_b [E_t(k)^2 - E^2] / [E_t(k)^2 - E^2],$$

where $E_t(k) = E_t + \hbar^2 k^2 / 2M$ and $E_c(k) = E_c + \hbar^2 k^2 / 2M$. Here, E and k are the energy and the wave vector of an excitonic polariton, $E_t = 1.8242$ eV, $E_c = E_t + 0.50$ meV (Ref. 7), $\epsilon_b = 8.4$ (Ref. 9), and $M = m_e + m_h = 0.58m_0$ (electron mass).⁹ From this dispersion relation, the density of states $D(E)$ is obtained to be $k^2 / (\pi^2 |dE/dk|)$. Therefore, the luminescence line shape of the A -LO band is proportional to the product of $D(E)$, $\exp(-E/k_B T_e)$ and $|V_F(q)|^2$ as follows:

$$I(\tilde{E} = E - E_{LO}) \propto \exp(-E/k_B T_e) D(E) (1/k)^2 \times \{1/[1 + (\alpha_e k)^2]^2 - 1/[1 + (\alpha_h k)^2]^2\}, \quad (2)$$

where

$$\alpha_{e(h)} = (a_B/2)m_{h(e)}/(m_e + m_h)$$

and q is replaced by k because $q \cong k$. The values of m_e , m_h , and a_B are $0.13m_0$, $0.45m_0$, and 53.6 \AA , respectively.¹⁰ The line shapes fitted on the basis of Eq. (2) are shown in Fig. 1 by dotted lines, assuming $T_e = 9$ K for (a) and 14 K for (b). The fitting is satisfactory. Using the same values of T_e , the line shapes of the A -2LO band were found to be also well explained by

$$I(\tilde{E} = E - 2E_{LO}) \propto \exp(-E/k_B T_e) D(E).$$

Therefore, the line-shape analysis on the basis of Eq. (2) is precise enough.

Energy- and time-resolved luminescence are shown in Figs. 2 and 3. These figures are constructed from the spectrally resolved temporal response of luminescence. It can be seen from the figures that the rise of the luminescence is determined by the time resolution of the instrument at the high-energy extremity (1.806 eV). On the other hand, it takes more than 300 ps for the luminescence intensity to reach its maximum below 1.799 eV. Excitons relax toward lower-energy states losing their energy.

The luminescence intensity of the A -LO band is related to the energy- and time-dependent distribution function $f(E, t)$ by the following equation:

$$I(\tilde{E} = E - E_{LO}, t) \propto f(E, t) D(E) (1/k)^2 \times \{1/[1 + (\alpha_e k)^2]^2 - 1/[1 + (\alpha_h k)^2]^2\}. \quad (3)$$

Using Eq. (3) and $I(\tilde{E}, t)$ which is directly displayed in Fig. 2, we can deduce $f(E, t)$. The obtained $f(E, t)$ was found to be approximately described by a Boltzmann distribution. The average energy and the total number of excitons $\langle E_e \rangle$ and N_e are calculated by

$$\langle E_e \rangle = \left[\sum_{i=-1}^8 E_i f(E_i, t) D(E_i) \right] / \left[\sum_{i=-1}^8 f(E_i, t) D(E_i) \right],$$

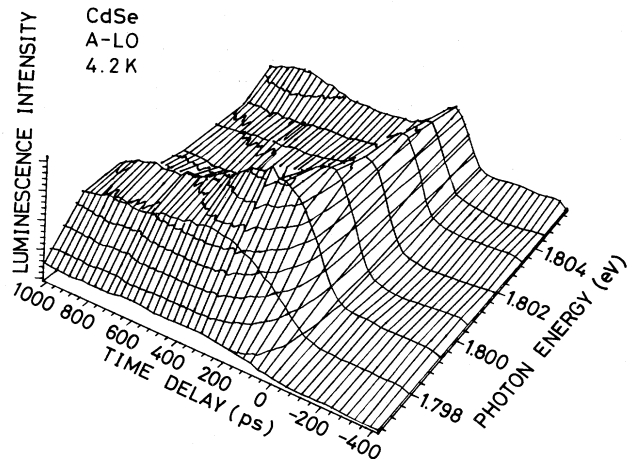


FIG. 2. Three-dimensional view of energy- and time-resolved luminescence intensity of the A -LO band in CdSe at 4.2 K.

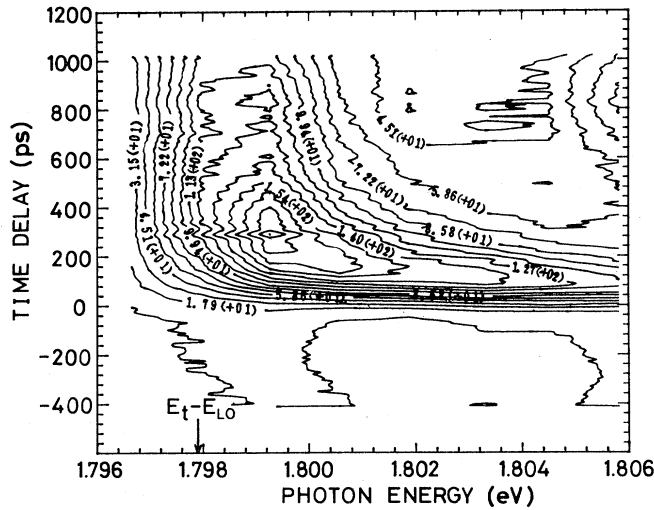


FIG. 3. Contour map of Fig. 2. Quantities in parentheses represent powers of ten by which the associated numbers are to be multiplied.

and

$$N_e = \sum_{i=1}^8 f(E_i, t) D(E_i) .$$

Here, E_i 's ($i=1-8$) minus E_{LO} are the photon energies where the temporal response of luminescence intensity is observed. The calculated $\langle E_e \rangle$ and N_e are shown in Fig. 4. The result indicates that excitons lose their energy at the time constant ~ 150 ps, which is much faster than their lifetime of 2.8 ns.

The kinetic energy loss rate of excitons can be calculated for three individual scattering processes: (i) the deformation-potential-type interaction with LA phonons; (ii) the piezoelectric-type interaction with LA or TA pho-

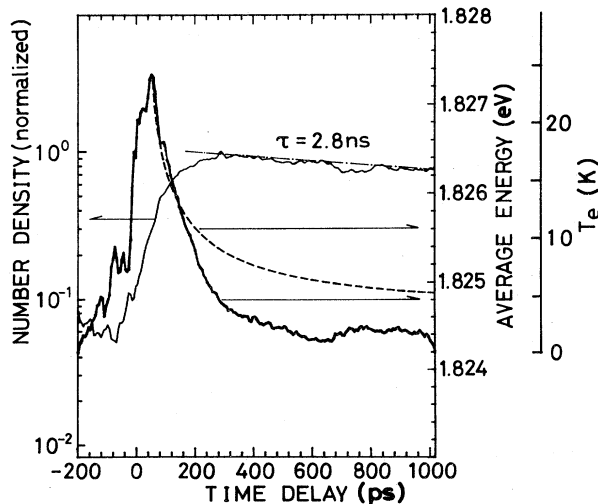


FIG. 4. Temporal change of the number density (a fine line) and the average energy (a bold line) of the A-exciton ensemble in CdSe at 4.2 K. The theoretical calculation on the basis of the model described in the text is shown by a dashed line.

nons; and (iii) the Fröhlich-type interaction with LO phonons. The matrix element of (iii) is given by Eq. (1), and those of (i) and (ii) are described by^{8,11}

$$V_{dp}(q) = (\hbar/2\rho u_L)^{1/2} q^{1/2} (D_c q_e - D_v q_h) ,$$

and

$$V_{pe}(q) = (\hbar/2\rho u_{L(T)})^{1/2} \times [4\pi e \langle e_{ij}^2 \rangle_{L(T)}^{1/2} / (\epsilon_0 q^{1/2})] (q_e - q_h) . \quad (4)$$

Here, $D_{c(v)}$ is the deformation potential of the conduction (valence) band, ρ the density, $\langle e_{ij}^2 \rangle_{L(T)}$ the spherical average of the squares of the piezoelectric constant for the LA (TA) phonons, and $u_{L(T)}$ the sound velocity of the LA (TA) phonons. Because the q dependence of $V_{dp}(q)$, $V_{pe}(q)$, and $V_F(q)$ are different from one another, the dominant energy-loss mechanism is alternated depending on the wave vector of excitons.

It is very difficult to derive the energy-loss rates of the excitons populated on the polariton dispersion using the exact forms of $V_{dp}(q)$, $V_{pe}(q)$, and $V_F(q)$. The derivation can be performed only numerically. On the other hand, we can derive the analytical expression for the energy-loss rates of the excitons populated on the parabolic dispersion, taking the asymptotic forms of the matrix elements. As mentioned above, we have precisely treated the experimental results to derive the time-resolved average energy of excitons. In the following theoretical analysis, however, we take the parabolic exciton dispersion for simplicity and for good insight. We derive the energy-loss rates of the exciton ensemble obeying the Maxwell-Boltzmann distribution. They are given by the following equations for $k < a_B^{-1} = 2$

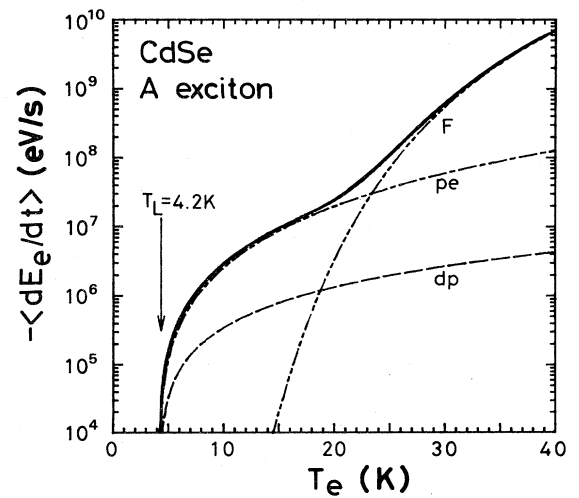


FIG. 5. Calculated energy-loss rates of excitons obeying the Maxwell-Boltzmann distribution with the exciton temperature T_e . Three individual energy-loss rates due to the deformation-potential-type, the piezoelectric-type, and the Fröhlich-type interactions are shown by a dashed line (dp), a dash-dotted line (pe), and a dash-double-dotted line (F), respectively. A bold solid line shows the total energy-loss rate which is a sum of the three individual loss rates.

$\times 10^6 \text{ cm}^{-1}$.

$$\left\langle \frac{dE_e}{dt} \right\rangle_{dp} = - \frac{2^{7/2} D^2 M^{5/2}}{\pi^{3/2} \hbar^4 \rho} (k_B T_e)^{3/2} \left(\frac{T_e - T_L}{T_e} \right), \quad (5)$$

$$\left\langle \frac{dE_e}{dt} \right\rangle_{pe} = - \frac{512 (2\pi)^{1/2} e^2 \langle e_{ij}^2 \rangle M^{7/2}}{\hbar^6 \epsilon_0^2 \rho} \times \left(\frac{m_e - m_h}{m_e + m_h} \right)^2 a_B^4 (k_B T_e)^{5/2} \left(\frac{T_e - T_L}{T_e} \right), \quad (6)$$

and

$$\left\langle \frac{dE_e}{dt} \right\rangle_F = - \frac{2^{1/2} e^2 M^{5/2} E_{LO}^{7/2}}{\hbar^6} \left(\frac{1}{\epsilon_\infty} - \frac{1}{\epsilon_0} \right) \left(\frac{m_e - m_h}{m_e + m_h} \right)^2 \times a_B^4 \left[\exp \left(- \frac{E_{LO}}{k_B T_e} \right) - \exp \left(- \frac{E_{LO}}{k_B T_L} \right) \right], \quad (7)$$

where $D = |D_c - D_v| = 2 \text{ eV}$ is the deformation potential of the A exciton,^{9,12} $T_L = 4.2 \text{ K}$ the lattice temperature, and $\langle e_{ij}^2 \rangle = \langle e_{ij}^2 \rangle_L + \langle e_{ij}^2 \rangle_T$. These equations can be derived following the same procedures as are described by Conwell,¹³ taking the asymptotic form ($q \rightarrow 0$) of the matrix elements of Eqs. (1) and (4). The numerical values of the parameters are $\rho = 5.81 \text{ g/cm}^3$, $\langle e_{ij}^2 \rangle_{L(T)} = 0.0144 \text{ C}^2/\text{m}^4$ (LA),

$0.0189 \text{ C}^2/\text{m}^4$ (TA),^{14,15} $\epsilon_0 = 9.70$,¹⁵ and $\epsilon_\infty = 7.02$.¹⁶ The calculated energy-loss rates by using Eqs. (5)–(7) are shown in Fig. 5.

The overall energy-loss rate $\langle dE_e/dt \rangle$ is given by the sum of $\langle dE_e/dt \rangle_{dp}$, $\langle dE_e/dt \rangle_{pe}$, and $\langle dE_e/dt \rangle_F$. Thus, the temporal trajectory of the $\langle dE_e/dt \rangle$ follows the curve of the overall energy-loss rate. Along this trajectory, the temporal change of $\langle E_e \rangle$ can be calculated with the initial temperature $T_e = 24.2 \text{ K}$, noting that $\langle E_e \rangle = E_i + (3/2)k_B T_e$. The calculated result is shown by the dashed line in Fig. 4. The agreement with experiment is good except at the low-energy region. The piezoelectric-type exciton-phonon interaction plays the predominant role in the energy relaxation of excitons. Furthermore, it should be noted from Fig. 4 that the experimental average energy is lowered below $E_i + (3/2)k_B T_L$ after 300 ps. This fact is not so surprising because excitons can be populated on the polariton dispersion even below E_i . Thus, it comes from the polariton effect. The numerical analysis taking account of the exact forms of $V_{dp}(q)$, $V_{pe}(q)$, and $V_F(q)$ as well as the polariton effect may give the full explanation of the experimental results. However, our essential conclusion concerning the energy-loss rates of excitons should still be valid. Instead, we should note that the simple calculation procedure mentioned above is useful to analyze the energy relaxation of excitons.

¹P. Wiesner and U. Heim, Phys. Rev. B **11**, 3071 (1975).

²Y. Masumoto and S. Shionoya, J. Phys. Soc. Jpn. **51**, 181 (1982).

³T. Kushida, S. Kinoshita, F. Ueno, and T. Ohtsuki, J. Phys. Soc. Jpn. **52**, 1838 (1983).

⁴F. Askary and P. Y. Yu, Phys. Rev. B **28**, 6165 (1983).

⁵E. Gross, S. Permogorov, and B. Razbirin, J. Phys. Chem. Solids **27**, 1647 (1966).

⁶V. A. Abramov, S. A. Permogorov, B. S. Razbirin, and A. I. Eki-mov, Phys. Status Solidi **42**, 627 (1970).

⁷C. Hermann and P. Y. Yu, Phys. Rev. B **21**, 3675 (1980).

⁸Y. Toyozawa, Progr. Theor. Phys. **20**, 53 (1958).

⁹F. Askary and P. Y. Yu, Solid State Commun. **47**, 241 (1983).

¹⁰B. Segall and D. T. F. Marple, in *Physics and Chemistry of II-VI Compounds*, edited by M. Aven and J. S. Prener (North-Holland,

Amsterdam, 1967), Chap. 3.

¹¹C. Weisbuch and R. G. Ulbrich, in *Light Scattering in Solids III*, edited by M. Cardona and G. Gütherodt (Springer, Berlin, 1982), p. 207.

¹²D. W. Langer, R. N. Euwema, K. Era, and T. Koda, Phys. Rev. B **2**, 4005 (1970).

¹³E. M. Conwell, in *Solid State Physics*, edited by F. Seitz, D. Turnbull, and H. Ehrenreich (Academic, New York, 1967), Suppl. 9, Chap. 3.

¹⁴A. R. Hutson, J. Appl. Phys. **32**, 2287 (1961).

¹⁵D. Berlincourt, H. Jaffe, and L. R. Shiozawa, Phys. Rev. **129**, 1009 (1963).

¹⁶R. E. Halsted, M. R. Lorenz, and B. Segall, J. Phys. Chem. Solids **22**, 109 (1961).